

Thermal Degradation and Bimolecular Decomposition of 2-Ethoxyethanol in Binary Ethanol and Isobutanol Solvent Mixtures: A Computational Mechanistic Study

Rima H. Al Omari,* Mansour H. Almatarneh,* Asmaa Y. Alnajjrah, Mohammed S. Al-Sheraideh, Sanaa S. Al Abbad, and Zainab H. A. Alsunaidi



Cite This: *ACS Omega* 2021, 6, 13365–13374



Read Online

ACCESS |



Metrics & More

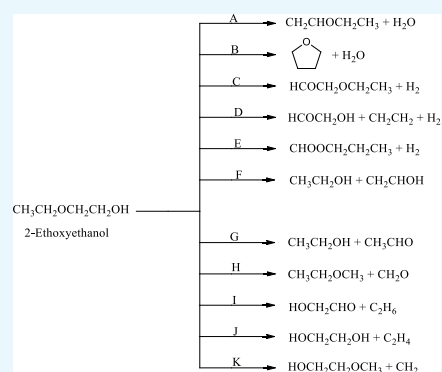


Article Recommendations



Supporting Information

ABSTRACT: A thorough computational study of a thermal degradation mechanism of 2-ethoxyethanol (2-EE) in the gas phase has been implemented using G3MP2 and G3B3 methods. The stationary point geometries were optimized at the B3LYP functional utilizing the 6-31G(d) basis set. Intrinsic reaction coordinate analysis was performed to determine the transition states on the potential energy surfaces. Nineteen primary different reaction mechanisms, along with the kinetic and thermodynamic parameters, are demonstrated. Most of the thermal degradation mechanisms result in a concerted transition state step as an endothermic process. Among 11 degradation pathways of 2-ethoxyethanol, the formation of ethylene glycol and ethylene is kinetically significant with an activation energy of 269 kJ mol^{-1} at the G3B3 method. However, the kinetic and thermodynamic calculations indicate that ethanol and ethanal's formation is the most plausible reaction with an activation barrier of 287 kJ mol^{-1} at the G3B3 method. For the bimolecular dissociation reaction of 2-ethoxyethanol with ethanol, the pathway that produces ether, H_2 , and ethanol is more likely to occur with a lower activation energy of 221 kJ mol^{-1} at the G3B3 method. Thus, 2-EE has experienced a set of complex unimolecular and bimolecular reactions.



1. INTRODUCTION

Alkoxyethanols are a significant class of materials from a logical perspective. Oxygenated compounds are progressively used as additives to gasoline products due to their octane-upgrading and contamination-reducing properties.¹ 2-Ethoxyethanol (2-EE) ($\text{C}_4\text{H}_{10}\text{O}_2$) is the ether alcohol formed by reacting ethylene oxide with ethyl alcohol.^{2,3} It is considered a natural volatile organic compound (VOC) known as ethylene glycol monoethyl ether (EGEE). It is an odorless, colorless solvent that has a sweet smell and a slightly bitter taste.^{2,3} It evaporates adequately, is flammable, and is soluble in water, ethanol, diethyl ether, acetone, and ethyl acetate.^{2–5} The chemical formula of 2-EE aids in its utilization as a solvent, industrial applications, and pharmaceutical procedures. Therefore, it is used in varnish removers, detergents, inks, resins, metal coatings, phenolic varnishes, cosmetics, and anti-freezing agents.⁶

Furthermore, 2-EE is an indirect biofuel filter because of its unique original synthesis mechanism from basic bioalcohols such as methanol and ethanol.^{5,7} It is also released from the chemical industry, where it is produced as a byproduct. As a VOC, 2-EE can be engaged with the arrangement of the ground-level ozone and yields harmful materials. However, emission of 2-EE is not expected to have any adverse effects on the worldwide environment.^{2,5,8} Evaluation of the risks to

human health and the environment occurs due to exposure to glycol ethers, such as 2-methoxyethanol, 2-ethoxyethanol, 2-methoxyethyl acetate, and 2-ethoxyethyl acetate. These glycol ethers are used as solvents with some applications in paints, stains, lacquers, and food-contact plastic production. Sections concerned with exposure sources note the significance of these solvents' evaporations and their overall emissions that have considerable potential for direct human vulnerability in manufacturing, small-scale workshops, and home during numerous consumer use products. The limited energy sources and the global natural effect of renewable energy consumption turned into a critical issue pushing to scan alternative fossil fuel sources.⁹ Bioethanol is the most popular biofuel due to its essential properties, such as water absorption, low internal energy, low combustion efficiency, high ignition temperature, and high vapor pressure. It would release dreadful discharges

Received: March 11, 2021

Accepted: April 29, 2021

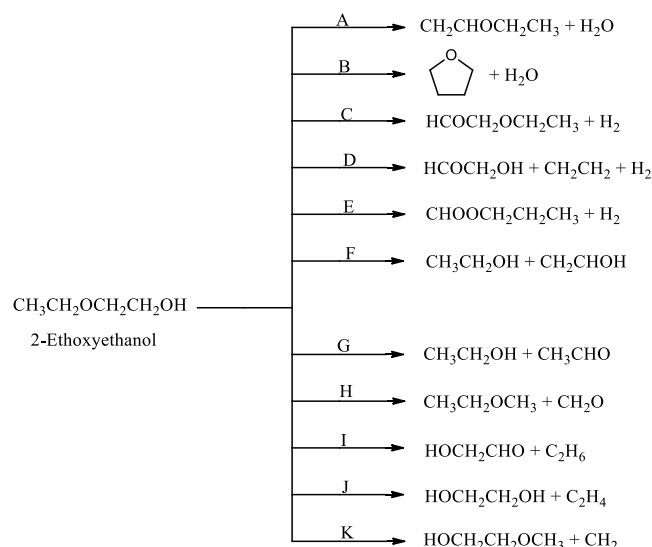
Published: May 12, 2021



to the atmosphere, affecting antagonistically the human health.^{10,11}

To the best of our information, there is no experimental or theoretical work related to 2-EE. Therefore, we are going to shed light on this subject by investigating the thermochemistry of 2-EE pyrolysis as biofuel additives. Scheme 1 illustrates the investigated reaction mechanisms herein for 2-EE unimolecular thermal degradation.

Scheme 1. Proposed Pathways for the Thermal Degradation of 2-Ethoxyethanol



The study of mixtures that include alkoxyethanols facilitates the investigation of self-association by inter- and intramolecular hydrogen bonds related to the presence of the oxygen atom and hydroxyl groups within the molecules.^{12,13} In detail, the formation of the intramolecular H-bonding improved dipole–dipole interactions in the mixtures of alkoxyethanols and alkanes compared to those present in mixtures with homomorphic alkanols. A thorough computational study is directed to reveal the possible reaction mechanism. The 11 potential possibilities of the unimolecular dissociation of 2-EE were investigated (Scheme 1). Furthermore, we studied the bimolecular reactions of 2-EE with

ethanol and isobutanol. Scheme 2 shows the proposed pathways for bimolecular decomposition in binary 2-EE with ethanol and isobutanol solvent mixtures. Thermodynamic and kinetic parameters were investigated at different levels of theory. This study's primary aim is to examine all the possible reaction mechanisms and determine the main favorable reaction routes. It is imagined that this computational study would hold any significance to experimentalists by giving thorough information about these reactions and offering a structure of new analyses for the improvement of valuable manufactured techniques.

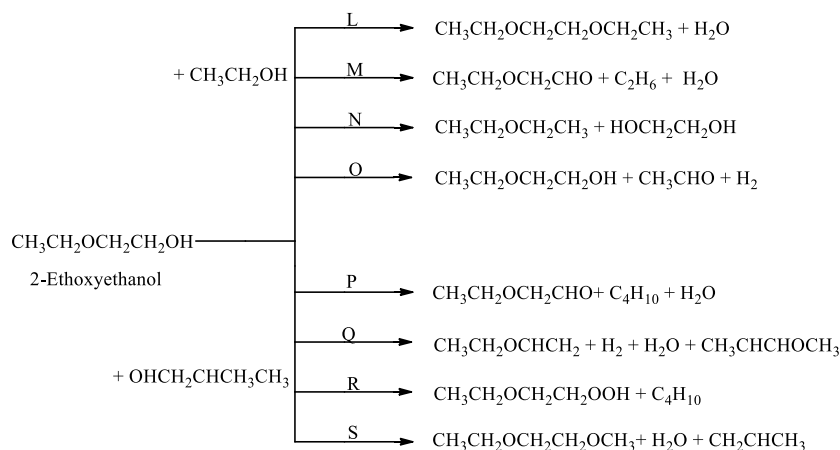
2. COMPUTATIONAL METHODS

All the electronic structure calculations were performed utilizing the Gaussian-16 (G16) package.¹⁴ The geometries of all reactants (Rs), transition states (TSs), intermediates (Is), and products (Ps) were fully optimized at the B3LYP functional^{15,16} utilizing the 6-31G(d) basis set.¹⁷ In this study, the energies and the enthalpies of the mechanisms were calculated utilizing Gaussian-*n* (G*n*) theories such as G3MP2 and G3B3. They have been selected based on their accuracy and the contrast between wave function and density functional theories that they provide.^{18–20} Normal mode analysis of frequencies was counted for all the proposed structures to ensure two things: first, the absence of imaginary frequencies in the minima; second, the presence of only one imaginary frequency in the transition states. The complete reaction pathways on the potential energy diagrams (PEDs) for all proposed mechanisms have been confirmed utilizing intrinsic reaction coordinate (IRC) analysis for all TSs. Structures at the last IRC points have been optimized and investigated to recognize the reactant and product to which each transition state is associated.²¹

3. RESULTS AND DISCUSSION

In this thorough study, comprehensive computational quantum chemistry calculations for 19 reaction pathway mechanisms were proposed for the thermal degradation of 2-EE. Pathways A → K include the unimolecular dissociation of 2-EE, as shown in Scheme 1 and Figures 1 and 3. Meanwhile, pathways L → S comprise the bimolecular reactions of 2-EE with other solvents such as ethanol and isobutanol, as depicted in Scheme 2 and Figures 5 and 6. It is worth observing that all thermal

Scheme 2. Proposed Pathways of the Bimolecular Reaction of Binary 2-Ethoxyethanol with Ethanol and Isobutanol Solvent Mixtures



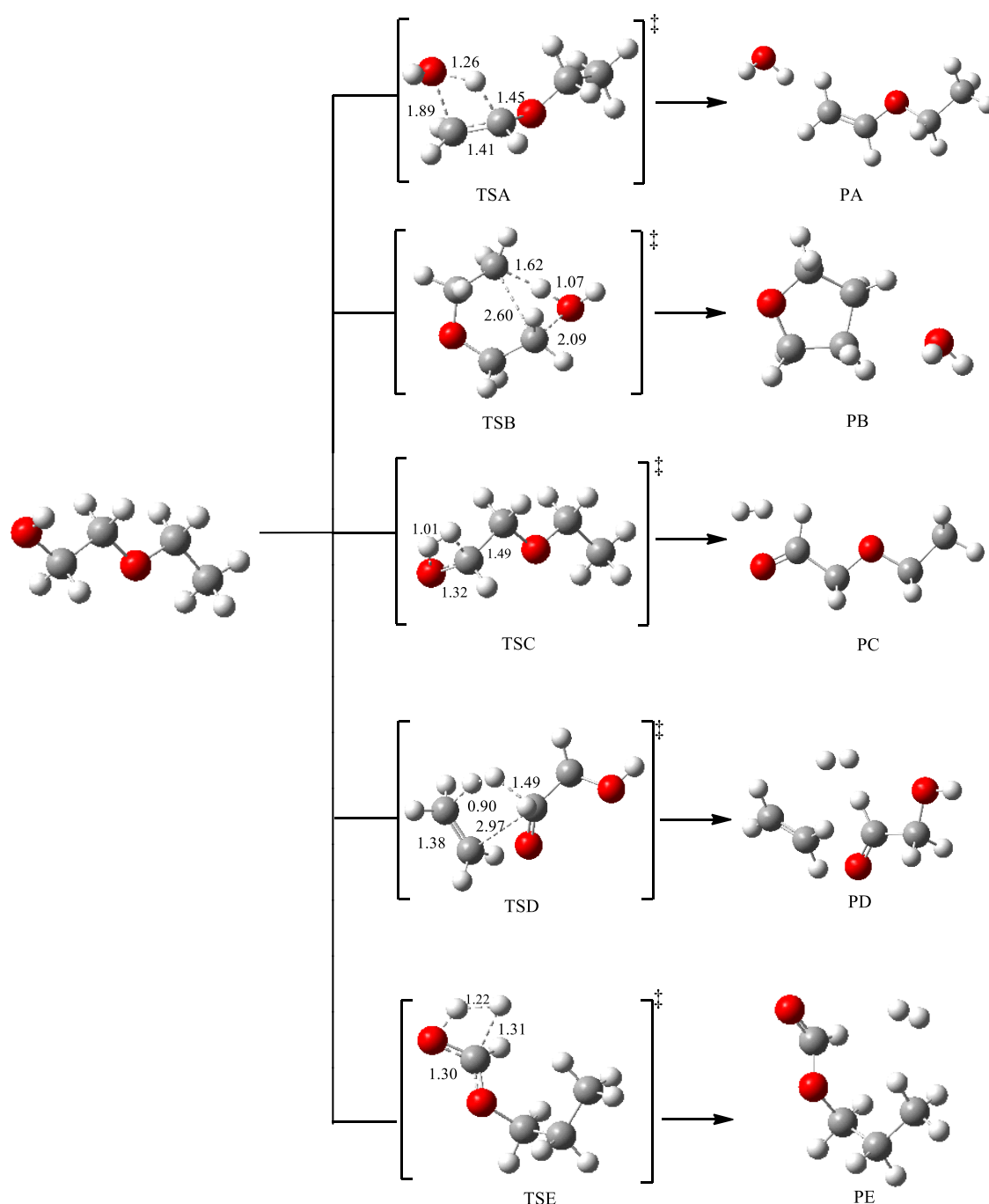


Figure 1. Proposed reaction mechanism pathways for the degradation of 2-EE (pathways A → E).

degradation reaction mechanisms occur in a concerted step as an endothermic process, excluding pathways B, E, G, and I, which are considered exothermic. The activation energies (E_a), enthalpies of activation (ΔH^\ddagger), and Gibbs energies of activation (ΔG^\ddagger) were calculated at different levels of theory (Tables 1–3) for all proposed pathways. The foremost favorable pathways were indicated utilizing the calculated kinetic energies; those with lower values are taken as the most reasonable. On the other hand, the stationary points are projected on PEDs for analogous pathways to distinguish the energies of the favorable reactions (Figures 2 and 4 and Figure S1 in the Supporting Information).

3.1. Unimolecular Dissociation of 2-EE. Two acceptable pathways for the dehydration step of 2-EE have been denoted

as pathways A and B. In the first transition state for pathway A (TSA), H_2O is eliminated from the carbon atom adjacent to the etheric oxygen of 2-EE to produce an unsaturated bond (Figure 1). In the second mechanism, the five-membered-ring transition state (TSB) is prevalent, resulting in tetrahydrofuran (THF) formation, as depicted in pathway B (Figure 1). The optimized structures for reaction coordinates for all proposed unimolecular dissociation of 2-EE are projected on potential energy diagrams (PEDs) at various levels of theory, as shown in Figures 2 and 4 and Figures S1 and S2 (in the Supporting Information).

In TSA, a notable geometric alteration can be spotted. For example, the C–O and C–H bonds are increased by about 0.35 and 0.47 Å, respectively. In addition, the H and O atoms

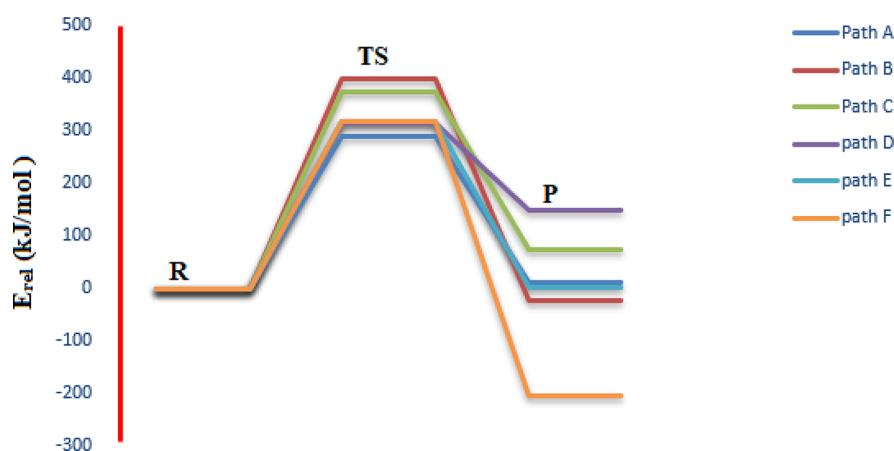


Figure 2. PED of the unimolecular dissociation reactions of 2-EE (pathways A \rightarrow F), calculated at the G3B3 method.

approach each other, and the gap between them appears to diminish by about 1.45 Å. The double bond has formed with a length of 1.41 Å. TSB demonstrates that the C–H and C–O bond lengths increase to 1.62 and 2.09 Å, respectively, and the H–O bond length diminishes to 1.07 Å. A single bond between C–C produced 2.60 Å due to forming a five-membered ring via THF.

Table 1 shows the activation energies (E_a) and Gibbs energies of activation for mechanism pathways A \rightarrow F. The TSA's activation energy (E_a) at the B3LYP/6-31G(d) level of theory is comparable with G3B3 with a value of 288 kJ mol⁻¹. For the G3MP2 method, the value deduced is 290 kJ mol⁻¹ (see Table 1). The TSB's activation energy is high compared to pathway A with a value of 388 kJ mol⁻¹ at the G3MP2 method and a value of 398 kJ mol⁻¹ at G3B3. The thermodynamic parameters show that pathway B is considered exothermic by 18 kJ mol⁻¹ and exergonic by 26 kJ mol⁻¹ at G3MP2 (Table S1). The formation of tetrahydrofuran (pathway B) is a thermodynamically favorable reaction; however, kinetically, it is not likely to occur. Therefore, it was of interest to study it in more detail at different theory levels, as illustrated in Table S1 in the Supporting Information. For TSB, the reported activation energies are 398 and 399 kJ mol⁻¹ at the G3B3 and APFD/6-31G(d) level of theory method, respectively. The lower activation energies have emerged at the G3MP2 method (Table 1 and Table S1). These barriers vary by only 36 kJ mol⁻¹ with the highest value at M11/6-31G(d) (424 kJ mol⁻¹) (Table S1). Nonetheless, these activation energies are still higher than pathway A.

Three pathways were studied and investigated to grasp the reaction mechanisms of the dehydrogenation process of 2-EE, denoted as pathways C, D, and E. All transition states are specified by two protons removable from particular sites in 2-EE. In comparison, pathway F indicated the removable ethanol mechanism. The highest barrier for TSC is 375 kJ mol⁻¹ at the G3B3 method, which is analogous to the results of the B3LYP/6-31G(d) level of theory and G3MP2 method. For TSD, the activation energy is 315 kJ mol⁻¹ at the G3MP2 method. Further, utilizing G3MP2 led to a rise in the energy barrier calculated value by no more than 10 kJ mol⁻¹. The same pattern of increasing the energy barrier was found with TSE and TSF (Table 1). The PED using the G3B3 method for pathways A \rightarrow F is depicted in Figure 2.

All the key bond lengths in TSF \rightarrow TSK are illustrated in Figure 3. The thermodynamic properties of pathways G and I

were constructed to be exothermic and exergonic at all methods, indicating that these reactions favor the forward direction. On the other hand, pathways H, J, and K were found to be endothermic and endergonic, and the reaction favors the reversible direction. The PED using the G3B3 method for pathways G \rightarrow K is depicted in Figure 4.

The formation of ethylene glycol and ethylene happens through the transition state TSJ (Figure 4). In pathway J, the H-atom of CH₃CH₂OCH₂CH₂OH approaches the etheric oxygen atom, and the C–H and C–C bonds are exceedingly prolonged. As a consequence, the strength of these bonds is considerably weakened. Contrariwise, the interaction of the O–H bond is intensified. The bond length between C–C bonds becomes longer and reaches 3.01 Å, consequently broken, and a double bond appears with a bond distance of 1.41 Å. The distance of the cracked C2–C3 bond is 2.98 Å. Eventually, ethylene glycol is produced by deducting the distance between O–H to 1.31 Å.

Pathway K represents the influence of photochemical interactions on the barrier. Therefore, chemical processes that comprise alkyl radicals have an essential effect on the disintegration of organic materials.²² Because most alkyl radicals are active and unstable,^{23,24} it is challenging to monitor their experimental methods. Thus, the mechanism of carbene formation is investigated through TSK. The ultraviolet light provokes 2-EE, which is considered weak, to undergo hemolytic cleavage to form methoxy ethanol and carbene.³¹ The energy barriers are deduced to be 518 and 520 kJ mol⁻¹ at the G3B3 and G3MP2 methods, respectively (Table 1). The B3LYP results conform to the values calculated at M11/6-31G(d), APFD/6-31G(d), and ω B97XD/6-31G(d) with a value of 526 kJ mol⁻¹ (Table S2). However, this reaction is not probable to happen due to the high activation energies. In this study, the most credible reaction mechanism kinetically is pathway J. The calculated energy barrier value at the G3B3 method is 269 kJ mol⁻¹ within a \pm 3 kJ mol⁻¹ difference from other levels of theory. Thermodynamically, pathway G will be the most plausible reaction mechanism. Carbene's production in pathway K is not a favorable channel, neither kinetically nor thermodynamically (Table 1 and Table S1).

Based on the data in Table 1, the activation energies show that the least costly computational-based method, B3LYP/6-31G(d), is an acceptable method for similar reactions. That is, activation energies calculated by B3LYP are within a 1–9 kJ mol⁻¹ difference for most pathways and about a 17–22 kJ

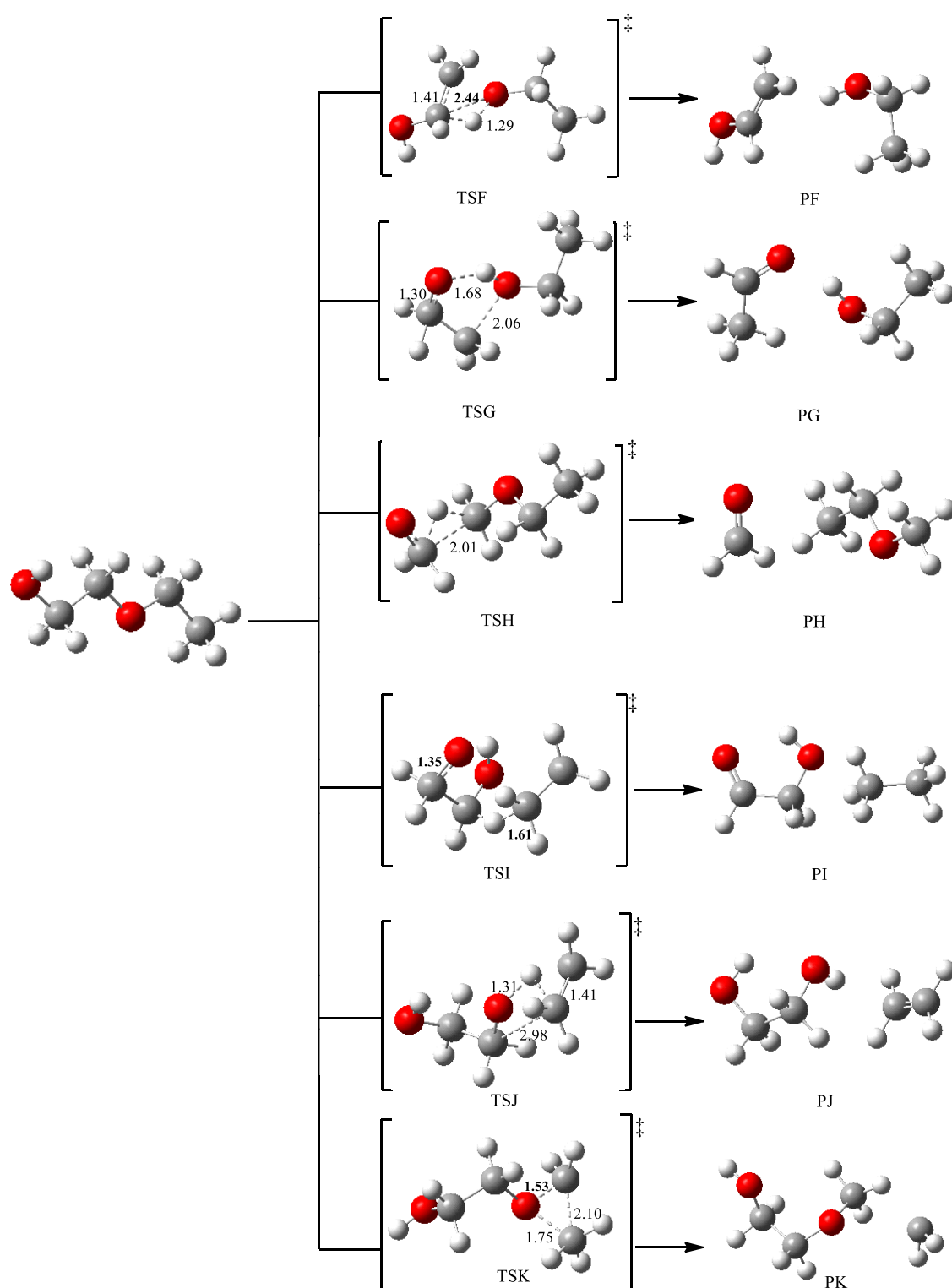


Figure 3. Proposed reaction mechanisms for the thermal degradation of 2-EE (pathways F → K).

mol^{-1} difference for pathways B, E, G, and I in comparison to the activation energy values computed using the more expensive computational methods such as Gaussian- n methods.

3.2. Bimolecular Dissociation of 2-EE. Mixtures containing hydroxy ethers are significant due to the substantial intermolecular impacts created by the existence of oxygen atoms and OH groups in the molecule (hydroxy ether).^{25,26}

Additionally, dipole moments of alkoxyethanols are higher than those of n -alkanols,²⁷ which produce vigorous dipole–dipole interactions. The study of binary liquid mixtures helps us understand the strength and nature of molecular interactions between the component molecules.^{28–30} In the present work, we broaden our investigations to the binary mixtures formed by 2-EE with two monoalcohols including ethanol and isobutanol at 298.15 K (see Scheme 2). Both

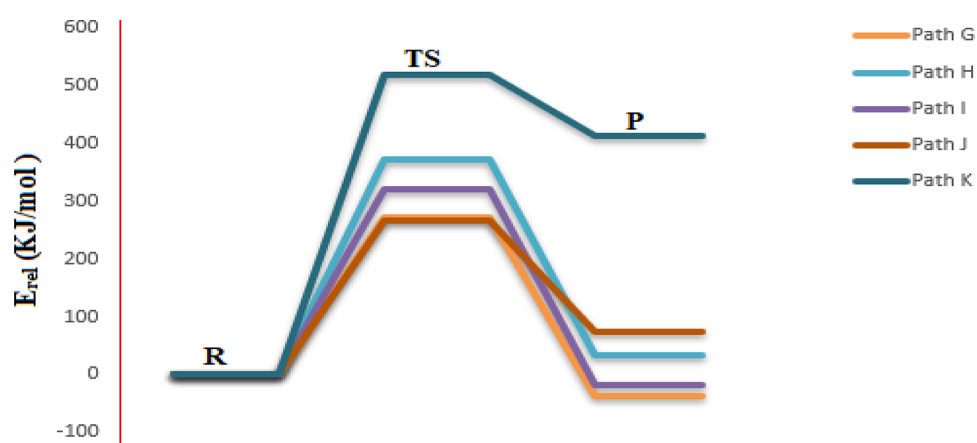


Figure 4. PED of the unimolecular dissociation reactions of 2-EE (pathways G \rightarrow K), calculated at the G3B3 method.

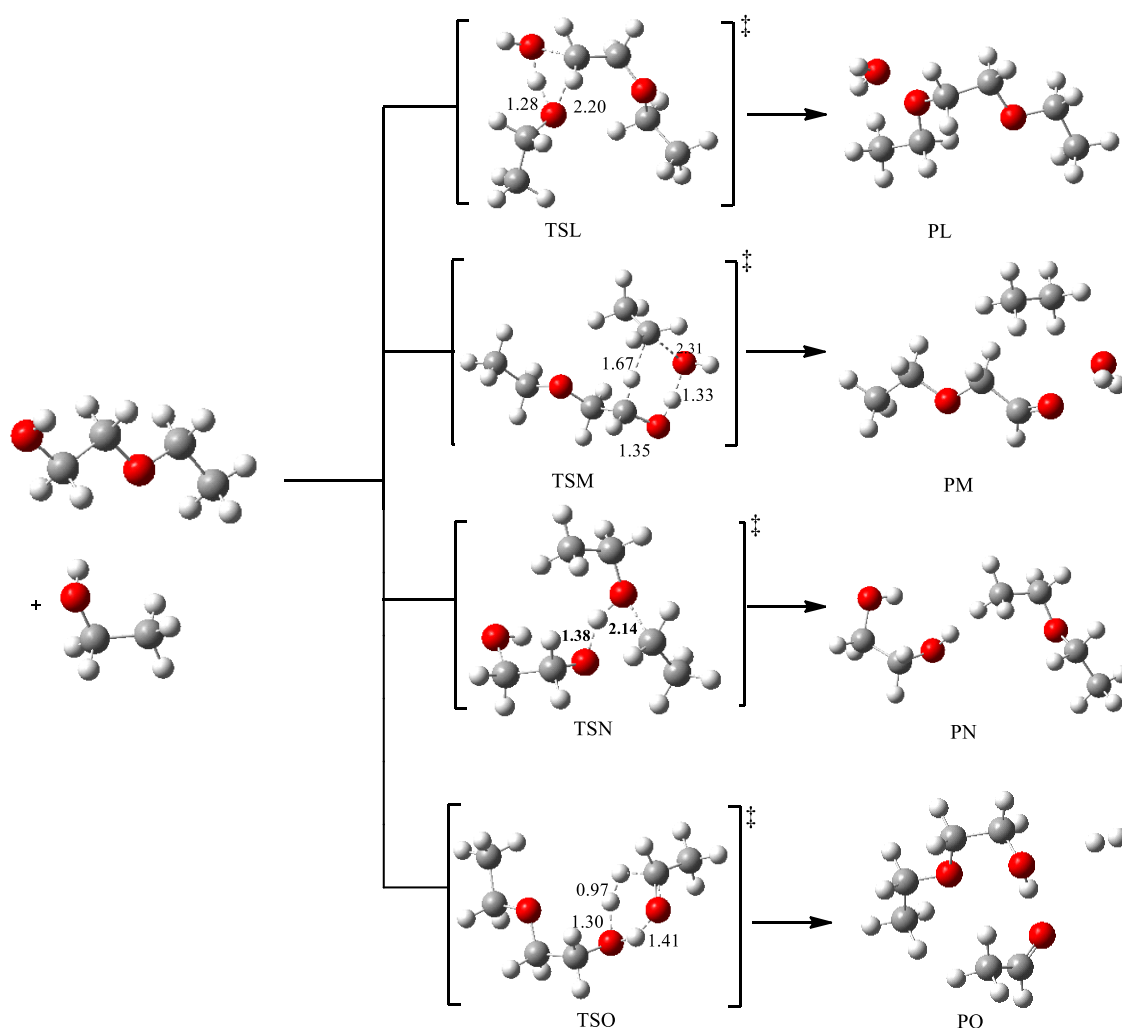


Figure 5. Proposed thermal degradation for reaction mechanisms of 2-EE (pathways L \rightarrow O).

thermodynamic functions (ΔH and ΔG), besides activation parameters (activation energies, E_a ; enthalpies of activation, ΔH^\ddagger ; and Gibbs energies of activation, ΔG^\ddagger), were calculated for all proposed pathways.

3.2.1. Reaction of 2-EE with Ethanol (Pathways L \rightarrow O). Four pathways were studied for the bimolecular reaction of 2-ethoxyethanol with ethanol (Scheme 2), which are pointed out as pathways L, M, N, and O. Figure 5 illustrates the

equilibrium geometries of all the stationary points that are included on the PED for pathways L \rightarrow O. The activation parameters such as energies and Gibbs energies for these reactions are shown in Table 2 and Figure 5. The water molecule is removed in both pathways L and M; also, ethane is removed in pathway M. Pathway N yields diethyl ether and 1,2-ethanediol. In contrast, in pathway O, a six-membered TSO is engaged and produces ether, H_2 , and ethanol. In TSL,

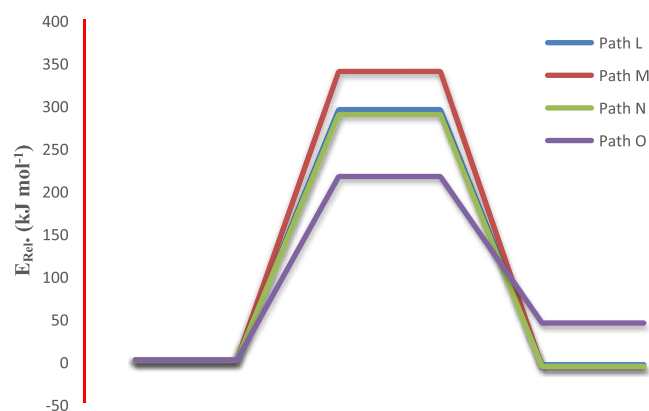


Figure 6. PED for the bimolecular dissociation of 2-EE for pathways L \rightarrow O. Relative energies at various calculation methods are reported in kJ mol^{-1} .

Table 1. Activation Energies (E_a) and Gibbs Energies of Activation (ΔG^\ddagger) for the Unimolecular Dissociation of 2-EE (in kJ mol^{-1}) at 298.15 K

transition states	B3LYP/6-31G(d)		G3MP2		G3B3	
	E_a	ΔG^\ddagger	E_a	ΔG^\ddagger	E_a	ΔG^\ddagger
TSA	288	288	290	289	289	289
TSB	405	410	388	386	398	404
TSC	376	375	375	375	375	375
TSD	306	305	315	316	316	316
TSE	298	298	311	314	317	317
TSF	287	284	291	286	290	288
TSG	273	274	292	291	287	288
TSH	372	370	381	381	381	379
TSI	321	327	343	347	342	348
TSJ	266	267	269	268	269	269
TSK	520	519	520	519	518	517

Table 2. Activation Energies (E_a) and Gibbs Energies (ΔG^\ddagger) of Activation for the Bimolecular Reaction of 2-EE with Ethanol (in kJ mol^{-1}) at 298.15 K

transition states	B3LYP/6-31G(d)		G3MP2		G3B3	
	E_a	ΔG^\ddagger	E_a	ΔG^\ddagger	E_a	ΔG^\ddagger
TSL	293	303	302	316	301	314
TSM	338	350	388	386	384	385
TSN	288	289	295	309	290	302
TSO	215	226	223	225	221	223

Table 3. Activation Energies and Gibbs Energies of Activation (E_a and ΔG^\ddagger) for the Bimolecular Reaction of 2-EE with Isobutanol (in kJ mol^{-1}) at 298.15 K

transition states	B3LYP/6-31G(d)		G3MP2		G3B3	
	E_a	ΔG^\ddagger	E_a	ΔG^\ddagger	E_a^\ddagger	ΔG
TSP	364	368	347	351	360	364
TSQ	351	352	349	351	348	389
TSR	438	435	433	430	431	429
TSS	446	445	448	447	451	450

the activation energies at G3B3 and G3MP2 are comparable, with 301 and 302 kJ mol^{-1} , respectively. Both methods'

activation energies are in good agreement with the B3LYP/6-31G(d) level of theory, differing by 9 kJ mol^{-1} .

Furthermore, the activation energies for TSM, TSN, and TSO at the G3B3 method are 384, 290, and 221 kJ mol^{-1} , respectively. Among these suggested pathways for the bimolecular reactions of 2-EE, pathway O is the most likely to occur. It has the lower barriers differing by 6 kJ mol^{-1} at different levels of theory (Figure 6). Moreover, the activation energies at the B3LYP/6-31G(d) level of theory are 288 and 215 kJ mol^{-1} , comparable with the corresponding value obtained at the G3B3 method (Table 2).

3.2.2. Reaction of 2-EE with Isobutanol (Pathways P \rightarrow S). The reactions of 2-EE with isobutanol were also considered computationally. Figure 7 depicts the proposed reaction mechanism for pathways P, Q, R, and S. Figure S3 (in the Supporting Information) shows the PED for pathways P \rightarrow S. Two proposed pathways (P and Q) include the 2-EE dehydration reaction. In Table 3, the activation energies and Gibbs energies of activation for pathways P \rightarrow S are reported. For TSP, the maximum activation energy is 364 kJ mol^{-1} calculated at the B3LYP/6-31G(d) level of theory, differing by 17 kJ mol^{-1} from the G3MP2 method. The activation energy of TSP at the G3B3 method is 360 kJ mol^{-1} . The lowest energy barrier among other transition states is TSQ, which is 351 kJ mol^{-1} at the B3LYP/6-31G(d) level of theory. The activation energies of TSR and TSS at the G3MP2 method are 433 and 448 kJ mol^{-1} , respectively, and are 431 and 451 kJ mol^{-1} at the G3B3 method, respectively. The values calculated using the G3B3 method perfectly match the corresponding values deduced at the B3LYP/6-31G(d) level of theory. It should be pointed out that the activation energies of the bimolecular reaction of 2-ethoxyethanol with ethanol (the lower barrier is 221 kJ mol^{-1} at the G3B3 method) are lower than those of the corresponding bimolecular reaction with isobutanol (the lower barrier is 348 kJ mol^{-1} at the G3B3 method).

4. THERMODYNAMIC PARAMETERS FOR THE DEGRADATION OF 2-ETHOXYETHANOL

The thermodynamic parameters (ΔH and ΔG) for the proposed unimolecular and bimolecular degradation reactions of 2-EE are investigated at all the former levels of theory and are listed in Table S3 in the Supporting Information. The degradation reactions of 2-EE are mostly endothermic and endergonic at all levels of theory. The unimolecular dissociation reactions of 2-EE (pathways B, E, G, and I) are exothermic and exergonic at all levels of theory. Considering the outcomes, we deduce that pathway G has the lowest thermodynamic parameter values; subsequently, it has more spontaneous and potential reactions.

5. CONCLUSIONS

A thorough computational study for the thermal degradation reaction of 2-ethoxyethanol has been executed in detail utilizing quantum chemical calculations. Eleven considerable pathways for the unimolecular reaction of 2-EE and eight for the bimolecular reactions with ethanol and isobutanol were studied extensively, with 19 pathways overall. The optimized geometries of Rs, TSs, Is, and Ps were determined. In addition, the potential energy diagrams (PEDs) were determined using the G3MP2 and G3B3 methods. The thermodynamic parameters (ΔH and ΔG) and the activation energies and

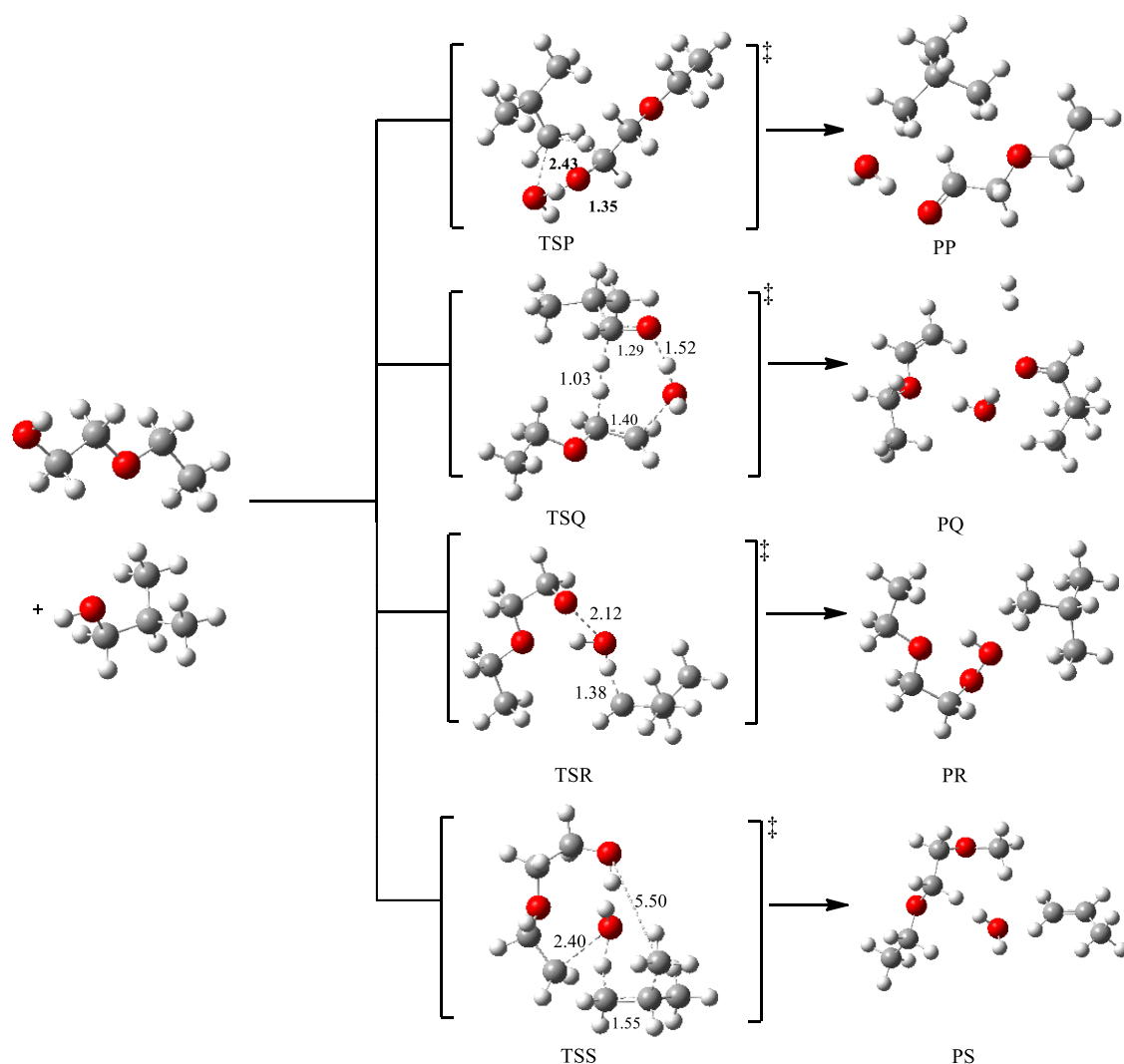


Figure 7. Proposed reaction mechanisms for the degradation of 2-EE (pathways P → S).

the Gibbs energies and enthalpies of activation (E_a , ΔG^\ddagger , and ΔH^\ddagger , respectively) were calculated using DFT and Gaussian- n theories for each proposed pathway. The TS of each pathway has been approved utilizing the intrinsic reaction coordinate (IRC) calculations. However, the reactions are firmly endothermic, excluding pathways B, E, G, I, L, M, and N pathways, where they are exothermic. The dehydration reaction is found by means of two different transition states, TSA and TSB, where the reactions are thermodynamically restrained. We have performed calculations using larger basis sets with B3LYP, ω B97XD, and APFD methods to investigate the effects of adding more polarization and diffuse functions. These levels of theory were used to calculate the activation energies and Gibbs energies of activation for the most significant pathways G, J, and K (the carbene formation). The calculated activation energies at these levels of theory were higher than the B3LYP results, as shown in Table S4 in the Supporting Information.

Several levels of theory have been used. We found that the energy values calculated at the B3LYP/6-31G(d) level of theory (least expensive computational method) are in agreement with the most costly computational methods such as Gaussian- n theories (G3MP2 and G3B3). Therefore, the B3LYP/6-31G(d) and B3LYP/6-311++G(3df,3pd) levels of

theory will be reliable and excellent options to study such systems in comparison with the costly computational methods. The optimized structures for all proposed pathways were very comparable at all levels of theory. We should also mention that the optimized structures for the most significant pathways G, J, and K were very close at all used levels of theory. Consequently, within the DFT formalism, adopting a higher basis set alters the geometries only very marginally (Table S4).

2-EE breaks down to create different products. Conformational alterations originated during the first TSs. The carbene formation pathway is energetically not preferable compared to all other pathways. Pathway K has the highest overall activation energy of 518 kJ mol⁻¹ at the G3B3 method. The formation of ethylene glycol and ethylene (pathway J) was found likely to occur for the unimolecular dissociation reactions of 2-EE as it has the lowest activation energy of 269 kJ mol⁻¹ at G3B3. Pathway O is more likely to occur for the bimolecular dissociation reactions with ethanol with a lower activation energy of 221 kJ mol⁻¹ at G3B3.

■ ASSOCIATED CONTENT

Supporting Information

The Supporting Information is available free of charge at <https://pubs.acs.org/doi/10.1021/acsomega.1c01318>.

Cartesian coordinates for all optimized structures of all proposed pathways along with thermodynamic and kinetic parameters and potential energy diagrams for selected pathways (PDF)

AUTHOR INFORMATION

Corresponding Authors

Rima H. Al Omari – *Pharmacological and Diagnostic Research Centre (PDRC), Faculty of Pharmacy, Al-Ahliyya Amman University, Amman 19328, Jordan;*
Email: r.alomari@ammanu.edu.jo

Mansour H. Almatarneh – *Department of Chemistry, University of Jordan, Amman 11942, Jordan; Department of Chemistry, Memorial University, St. John's, NL A1B 3X7, Canada;*  orcid.org/0000-0002-2863-6487;
Phone: (+962) 790182748; Email: m.almatarneh@ju.edu.jo

Authors

Asmaa Y. Alnajjrah – *Department of Chemistry, University of Jordan, Amman 11942, Jordan*

Mohammed S. Al-Sheraideh – *Department of Chemistry, College of Science, Imam Abdulrahman Bin Faisal University, Dammam 31441, Saudi Arabia*

Sanaa S. Al Abbad – *Department of Chemistry, College of Science, Imam Abdulrahman Bin Faisal University, Dammam 31441, Saudi Arabia*

Zainab H. A. Alsunaidi – *Department of Chemistry, College of Science, Imam Abdulrahman Bin Faisal University, Dammam 31441, Saudi Arabia*

Complete contact information is available at:

<https://pubs.acs.org/10.1021/acsoomega.1c01318>

Notes

The authors declare no competing financial interest.

ACKNOWLEDGMENTS

M.H.A. is grateful to the Deanship of Academic Research at the University of Jordan for the grant. We acknowledge the ACEnet and Compute Canada for computer time.

REFERENCES

- (1) Zéberg-Mikkelsen, C. K.; Lugo, L.; García, J.; Fernández, J. Volumetric properties under pressure for the binary system ethanol + toluene. *Fluid Phase Equilib.* **2006**, *2*, 139–151.
- (2) World Health Organization 2-Methoxyethanol, 2-ethoxyethanol, and their acetates; World Health Organization (WHO): 1990.
- (3) Johnson, W., Jr. Final Report on the Safety Assessment of Ethoxyethanol and Ethoxyethanol Acetate. *Int. J. Toxicol.* **2002**, *21*, 9–62.
- (4) Abdel-Rahman, M. A.; Al-Hashimi, N.; Shibl, M. F.; Yoshizawa, K.; El-Nahas, A. M. Thermochemistry and Kinetics of the Thermal Degradation of 2-Methoxyethanol as Possible Biofuel Additives. *Sci. Rep.* **2019**, *9*, 4535.
- (5) *Glycol Ethers 2-Methoxyethanol and 2-Ethoxyethanol*; DHHS (NIOSH) Publication: 1983, 39, 83–112.
- (6) Kohse-Höinghaus, K.; Oßwald, P.; Cool, T. A.; Kasper, T.; Hansen, N.; Qi, F.; Westbrook, C. K.; Westmoreland, P. R. Biofuel combustion chemistry: from ethanol to biodiesel. *Angew. Chem., Int. Ed.* **2010**, *49*, 3572–3597.
- (7) Yue, H.; Zhao, Y.; Ma, X.; Gong, J. Ethylene glycol: properties, synthesis and applications. *Chem. Soc. Rev.* **2012**, *41*, 4218–4244.
- (8) Ye, L.; Zhao, L.; Zhang, L.; Qi, F. Theoretical studies on the unimolecular decomposition of Ethylene Glycol. *J. Phys. Chem. A.* **2012**, *116*, 55–63.
- (9) Shafiee, S.; Topal, E. When will fossil fuel reserves be diminished. *Energy Policy.* **2009**, *37*, 181–189.
- (10) Jacobson, M. Z. Effects of Ethanol (E85) versus Gasoline Vehicles on Cancer and Mortality in the United States. *Environ. Sci. Technol.* **2007**, *41*, 4150–4157.
- (11) Gogoi, B.; Raj, A.; Alrefaai, M. M.; Stephen, S.; Anjana, T.; Pillai, V.; Bojanampati, S. Effects of 2,5-dimethylfuran addition to diesel on soot nanostructures and reactivity. *Fuel* **2015**, *159*, 766–775.
- (12) González, J. A.; Cobos, J. C.; Javier Carmona, F. J.; De La Fuente, I. G.; Bhethanabotla, V. R.; Campbell, S. W. Thermodynamics of mixtures containing alkoxyethanols. Part XV. DISQUAC characterization of systems of alkoxyethanols with n-alkanes or cyclohexane. *Phys. Chem. Chem. Phys.* **2001**, *3*, 2856–2865.
- (13) Mozo, I.; De La Fuente, I. G.; González, J. A.; Cobos, J. C. Thermodynamics of Mixtures Containing Alkoxyethanols. XXIV. Densities, Excess Molar Volumes, and Speeds of Sound at (293.15, 298.15, and 303.15) K and Isothermal Compressibilities at 298.15 K for 2-(2-Alkoxyethoxy) ethanol + 1-Butanol Systems. *J. Chem. Eng. Data* **2007**, *52*, 2086–2090.
- (14) Frisch, M. J.; Trucks, G. W.; Schlegel, H. B.; Scuseria, G. E.; Robb, M. A.; Cheeseman, J. R.; Scalmani, G.; Barone, V.; Petersson, G. A.; Nakatsuji, H.; Li, X.; Caricato, M.; Marenich, A. V.; Bloino, J.; Janesko, B. G.; Gomperts, R.; Mennucci, B.; Hratchian, H. P.; Ortiz, J. V.; Izmaylov, A. F.; Sonnenberg, J. L.; et al. *Gaussian 16*; 2016.
- (15) Becke, A. Density-functional thermochemistry III The role of exact exchange. *J. Chem. Phys.* **1993**, *98*, 5648.
- (16) Lee, C.; Yang, W.; Parr, R. G. *Phys. Rev. B* **1988**, *37*, 785.
- (17) Hehre, W. J.; Ditchfield, R.; Pople, J. A. Self-consistent molecular orbital methods. XII. Further extensions of gaussian-type basis sets for use in molecular orbital studies of organic molecules. *J. Chem. Phys.* **1972**, *56*, 2257.
- (18) Curtiss, L. A.; Redfern, P. C.; Raghavachari, K.; Rassolov, V.; Pople, J. A. Gaussian-3 theory using reduced Moller-Plesset order. *J. Chem. Phys.* **1999**, *110*, 4703–4709.
- (19) Baboul, A. G.; Curtiss, L. A.; Redfern, P. C.; Raghavachari, K. Gaussian-3 theory using density functional geometries and zero-point energies. *J. Chem. Phys.* **1999**, *110*, 7650–7657.
- (20) Rassolov, V. A.; Ratner, M. A.; Pople, J. A.; Redfern, P. C.; Curtiss, L. A. 6-31G* basis set for third-row atoms. *J. Comput. Chem.* **2001**, *22*, 976–984.
- (21) Fukui, K. The path of chemical reactions - the IRC approach. *Acc. Chem. Res.* **1981**, *14*, 363.
- (22) Vereecken, L.; Nguyen, T. L.; Hermans, I.; Peeters, J. Computational study of the stability of α -hydroperoxyl- or α -alkylperoxyl substituted alkyl radicals. *Chem. Phys. Lett.* **2004**, *393*, 432–436.
- (23) Coppinger, G. M.; Swalen, J. D. Electron Paramagnetic Resonance Studies of Unstable Free Radicals in the Reaction of t-Butyl Hydroperoxides and Alkylamines. *J. Am. Chem. Soc.* **1961**, *83*, 4900–4902.
- (24) Rosenbaum, J.; Symons, M. C. R. Unstable intermediates. *Mol. Phys.* **1960**, *3*, 205–217.
- (25) Arroyo, F. J.; Carmona, F. J.; De La Fuente, I. G.; González, J. A.; Cobos, J. C. Excess Molar Volumes of Binary Mixtures of 1-Heptanol or 1-Nonanol with n-Polyethers at 25°C. *J. Solution Chem.* **2000**, *29*, 743–756.
- (26) Brinkley, R. L.; Gupta, R. B. Intra- and Intermolecular Hydrogen Bonding of 2-Methoxyethanol and 2-Butoxyethanol in Hexane. *Ind. Eng. Chem. Res.* **1998**, *37*, 4823–4827.
- (27) Riddick, J. A.; Bunger, W. B.; Sakano, T. K. *Organic solvents: physical properties and methods of purification*. Fourth edition. United States: N. p., 1986. Web
- (28) García, B.; Alcalde, R.; Leal, J. M.; Matos, J. S. Formamide-(C1–C5) alkan-1-ols solvent systems. *J. Chem. Soc., Faraday Trans.* **1996**, *92*, 3347–3352.

(29) Maham, Y.; Liew, C.-N.; Mather, A. E. Viscosities and Excess Properties of Aqueous Solutions of Ethanolamines from 25 to 80°C. *J. Solution Chem.* **2002**, *31*, 743–756.

(30) Ali, A.; Abida, H. S.; Nain, A. K. Molecular Interaction in Binary Mixtures of Benzyl Alcohol with Ethanol, Propan-1-ol and Octan-1-ol at 303 K: An Ultrasonic and Viscometric Study. *Czechoslov. Chem. Commun.* **2002**, *67*, 1125–1140.

(31) Abu-Saleh, A. A.-A. A.; Almatarneh, M. H.; Poirier, R. A. Bimolecular reactions of carbenes: Proton transfer mechanism. *Chem. Phys. Lett.* **2018**, *698*, 36–40.